Panamerican Mathematical Journal
ISSN: 1064-9735
Vol 33 No. 2 (2023)

FEA of Bajaj Discover 100 cc Connecting Rod for Aluminum Material

Dr. Prathamesh S. Gorane[1], Dr. Ritesh S. Fegade[2], Prof. Nehe Sandip Sampat[3], Dr. Vijay B. Roundal[4], Dr. Gulab Dattrao Siraskar[5], Dr. Pallavi Sachin Patil[6], Dr. Subhash Gadhave[7], Dr Vijaykumar K Javanjal[8]

[1, 2, 4] Assistant Professor, Department of Mechanical Engineering, GS Moze COE, Pune, India

[3] Assistant professor, Samarth College of engineering, Belhe, India

[5] Associate professor, Pimpri chinchwad college of engineering and research, Ravet, Pune, India

[6] Assistant Professor, Department of Computer Engineering, GS Moze COE, Pune, India

[7, 8] Associate professor, Department of Mechanical Engineering, Dr.D. Y. Patil Institute of Technology Pimpri Pune 18

Article History:

Received: *25-03-2023*

Revised: *20-05-2023*

Accepted: *05-06-2023*

Abstract:

The connecting rod is a vital component of internal combustion engines, responsible for converting the piston's linear motion into rotational motion. Its design involves careful consideration of material selection, geometry, and load distribution to ensure it can withstand the dynamic forces and stresses encountered during engine operation. Finite element analysis plays a crucial role in evaluating the structural performance of the connecting rod, allowing engineers to optimize its design for maximum efficiency and reliability. By understanding the complexities of connecting rod design and the forces acting upon it, engineers can develop robust and high-performing engines that meet the demands of modern automotive applications.

The paper describes a case study that was crucial to the engine development program's evaluation of the connecting rod's strength and fatigue analysis for Bajaj Discover 100 cc engine. The basic model was prepared using appropriate modeling software and then it was analyzed in Ansys for strength and fatigue analysis. The compressive and tensile loading was applied on the both ends of the connecting rod and the results were found. The location of the maximum stress was found.

Keywords: IC Engine, Connecting Rod, Material, FEA, Stress, Strain, Design.

1. Introduction

The connecting rod is a critical component in internal combustion engines, playing a pivotal role in transforming the linear motion of the piston into the rotational motion required to drive the crankshaft. As an essential element of the engine’s mechanical architecture, the connecting rod is subject to various forces and stresses that influence its design and performance. This comprehensive introduction will delve into the connecting rod's significance, its design considerations, the forces acting upon it, and the application of finite element analysis (FEA) in its evaluation.

In an internal combustion engine, the connecting rod connects the piston to the crankshaft, enabling the conversion of the piston's linear motion into the rotational motion needed to propel the vehicle.

This transformation is essential for the engine's functionality, as it allows the combustion process's energy to be effectively transmitted and utilized. The connecting rod must withstand significant loads and stresses during the engine's operation, making its design and material selection crucial for durability and performance.

Designing a connecting rod involves several key considerations to ensure it can withstand the operational demands of an internal combustion engine. The primary goals in designing a connecting rod include minimizing weight, maximizing strength, and ensuring durability under cyclic loading conditions. These objectives require careful attention to the following aspects:

Material Selection: The material used for the connecting rod must possess high strength-to-weight ratio, fatigue resistance, and good machinability. Common materials include forged steel, aluminum alloys, and titanium alloys. Each material offers distinct advantages and trade-offs in terms of weight, strength, and cost.

Geometry: The geometry of the connecting rod influences its strength and stiffness. Typically, connecting rods have an I-beam or H-beam cross-sectional profile, which provides an optimal balance between weight and structural integrity. The dimensions of the connecting rod, including length, width, and thickness, are carefully calculated based on the engine's specifications and performance requirements.

Load Distribution: The connecting rod must evenly distribute the forces it experiences during the engine's operation. Proper load distribution helps prevent localized stress concentrations, reducing the risk of fatigue failure. The design should ensure a smooth transition of forces from the piston to the crankshaft.

The connecting rod experiences various types of stress and strain during the engine's operation, including tensile, compressive, and bending stresses. These stresses arise from the dynamic forces generated by the piston's motion and the combustion process. Understanding these forces is crucial for designing a connecting rod that can withstand the operational conditions without failure.

2. Literature Review

[01] Mr. Yogesh Bharti et al. (2013),

Analyzed; connecting rod with help of ANSYS package. Human desired fulfilled by design process. As connecting rod is working in complicated condition, it is very complex design of connecting rod. To with stand different forces & stress connecting rod designed for best & suitable design. By using ANSYS, software FEA suggested minimum design specification. For same purpose PRO/ENGINEER WILDFIRE, software used to develop solid modeling & ANSYS software for its analysis.

With help of optimization process, best results & best-suited options provided. Reducing size & weight comparison of connecting rod by FEA affects performance of connecting rod.

[02] Mr. Yogesh R. Kchrola et al. (2017),

For selected material, FEA of connecting rod performed. Usually connecting rods produced with material carbon steel. Now day’s aluminium alloys also used for production of connecting rod. For improving mechanical properties of connecting rod, composite materials are used. The best synthesis

of parameters such as deformation, von misses strain & stress, weight reduction & factor of safety criticized by changed of material. The most important aspect in process is fatigue strength. Load acting on connecting rod was determined.

[03] Mr. Yong Wang et al. (2017),

Investigated; mechanical properties & process parameters on microstructures of liquid squeeze casting process & Semisolid squeeze casting for fabricating ZL104 connecting rod. Elongation of SSSC fabricated rods improved by 17% & tensile strength improved by 22% as compared with LSC fabricated rod. By rising re-melting temperature, shape factor as well as average particle size increased for SSSC.

On contrary elongation & tensile strength improved first & then lowered. With increasing mold temperature The APS was increased. On contrary SF greater than before firstly, then decreased because of which elongation & tensile strength increase firstly & then decrease. As squeezing pressure increased, SF increased & APS decreased, overall mechanical properties were improved.

[04] Mr. Yoo (1984),

Utilized verity condition flexibility, material subordinate thought of continuum mechanics as well as adjoint variable method for getting figure shape plan senses of stress. The outcomes utilized in an iterative advancement calculation, steepest plunge calculation, to mathematically, take care of an ideal plan issue.

The emphasis was on shape plan, affectability analysis with application to case of connecting rod. The pressure imperatives forced on chief worries of latency & terminating loads.

In any case, exhaustion quality not tended to. The other requirement was one on thickness to tie it away from zero. They could acquire 20% weight decrease in neck locale of connecting rod.

[05] Mr. Zhiwei Tong et al. (2009),

Processed; vibration mode shapes & modular appropriation subsequent to getting mode shapes & expository frequencies of three-dimensional FEA modular of connecting rod. Powerless pieces of complex mechanical framework & vibration mode shapes are controlled by Modal analysis is an adequately. Utilization of ideal elements plan strategy for mechanical structure framework performed rather than experience simple technique.

In process of drilling, reciprocating mud pump transports water or mud during drilling process. A modal analysis performed for improving reciprocating pump’s performance & decreasing failure of connecting rod because of vibrations during pump is in running condition. For future reference, weakness of connecting rod had provided reference point for structural optimization & dynamic analysis.

[06] Mrs. Dipalee S. Bedse (2017),

Evaluated design with FEA of connecting rod used in Hero Honda Engine Cycle for fatigue life. Connecting rod is main member of an IC engine also it keeps on moving repeatedly. Using FEA techniques connecting rod analyzed for its structural systems.

A FEA model was developed using CATIA software firstly, then FEA was carried out using HYPERMESH software to find out displacement & stresses in existing design of connecting rod under certain loading condition. For tensile loading UTM used for verifying structural strength of connecting rod. Best alternative design for connecting rod recommended considering load investigation result & observations of static FEA.

[07] Mrs. Dipalee S. Bedse et al. (2015),

From study, it seen that test conducted on UTM & FEA had shown similar result for deflection, stresses. In line with same, maximum stress, concentration observed at oil-hole portion at piston end & at neck radius of crank. Small changes, in geometry of connecting rod; done for improving fatigue life.

The halfway segment, between wrench and cylinder, known as, is associating pole. Interfacing pole otherwise called connecting rod and utilized to associate the cylinder to driving rod. As an associating bar is unbending, it might send either a push or a force thus the pole turns the wrench through the two parts of an unrest, for example cylinder pushing and cylinder pulling. Prior instruments, for example, chains, could just draw. In two or three two-phase motors, the interfacing bar simply needed to push. Today, associating poles are most popular through their utilization in inward burning cylinder motors, for example, car motors.

These are of a particularly unique plan from prior types of associating poles, utilized in steam motors and steam trains. One wellspring of energy in car industry is inside burning motor. Inner burning motor proselytes substance energy into Mechanical energy through responding movement of cylinder. Driving rod and Connecting bar convert responding movement into turning movement. Associating bar is one of the significant driving pieces of Light vehicle motor it shapes a basic instrument that changes over direct movement into rotational movement that implies the interfacing bar utilized to move straight, responding effort of cylinder into revolving movement of the crankshaft.

3. Methodology

Step 1: In depth study of connecting rod used for Bajaj Discover 100cc bike for aluminum material

Step 2: Define Input parameters for aluminum material

Step 3: Modeling exiting geometry for aluminum material

Step 4: Calculation of different forces acting on original design for aluminum material

Step 5: Selection of aluminum material

Step 6: Meshing & Applying Boundary conditions for aluminum material

Step 7: Finite Element Analysis of original design for Aluminum material

Static Analysis of Original Design for connecting rod used in Discover 100cc

The present connecting rod design involves of I cross-section at shank portion. Input considerations defined as mentioned below. The present mass of connecting rod is 0.099 kg. The calculations for present design are as followed.

Input parameters for design calculations of Original Discover Connecting Rod

Bore diameter	D	= 47 mm
Crank radius	R	= 27.2 mm
Crank speed	N	= 2000 RPM
Firing angle	θ	= 90 - 110
Length of connecting rod	L	= 92 mm
Maximum gas pressure	Pmax	= 2 MPa.
Weight of reciprocating masses	Mr	= 0.474 Kg

Specifications of Material

Material		= **Aluminium 360**
Density		= 2.63 g/cm3
Coefficient of Thermal Expansion		= 21 µm/m°K
Specific Heat		= 944 J/kg.K
Thermal Conductivity		= 113 (w/mK)
Resistivity		= 2.69 Ω.cm
Compressive Yield Strength		= 170 (MPa)
Tensile Yield Strength		= 170 (MPa)
Tensile Ultimate Strength		= 370 (MPa)
Compressive Ultimate Strength		= 370 (MPa)
Poisson's ratio	µ	= 0.33
Young's Modulus	E	= 88.5 GPa

Geometry of Original Discover Connecting Rod:

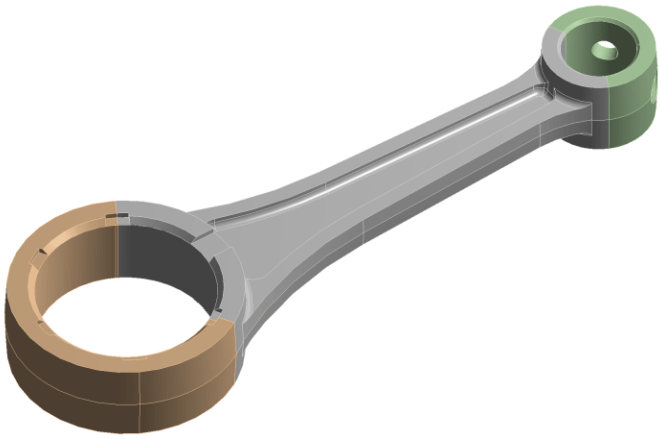

Figure 1: Geometry of Original Discover Connecting Rod

A solid model of discover connecting rod as observed in diagram was genrated using appropriate modeling software package i.e. Catia V5 modeler. From diagram, it can be seen that conncting rod is symmetric about axis line joining centres of gudgeon pin & crack end. Therefore connecting rod has modeled as symmetric model with the help of suitable modeling software i.e. Catia V5 modeler. The volume of connecting rod is 11873.2 mm^3 whereas mass of connecting rod is 0.099 kg.

Meshed Geometry of Original Discover Connecting Rod

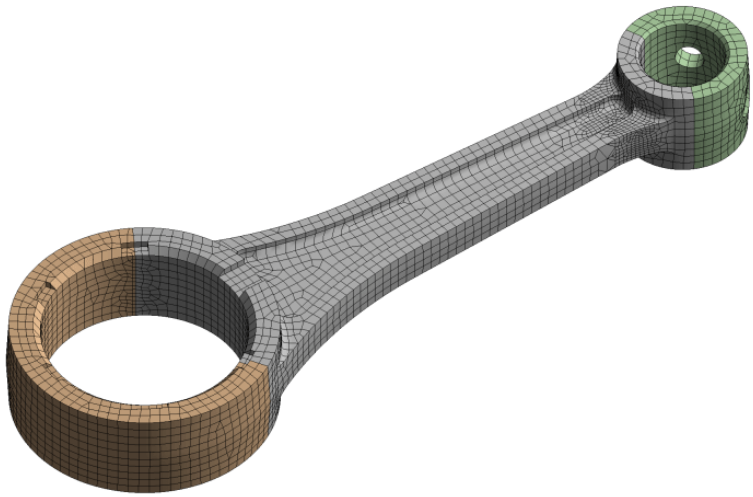

Figure 2: Meshed Geometry of Original Discover Connecting Rod

The figure shows Meshed model of discover Connecting rod prior to optimization. Finite Eement Analysis was done in Ansys 19 software. Finite element mesh was generated using hexahedral elements with maximum face size as 1.5 mm & number of elements or cells are 15920 with 55405 no. of nodes. Coarse meshing performed for reducing computational time. Purpose of selecting hexahedral element was to have better accuracy & better result for fatigue life estimation. According to four load cases, the boundary condition were applied.

Grid sensitivity analysis performed for the selection of the optimum cell size. The cell size was selected as mentioned ablove from the graph obtained from the grid sensitivty analysis. From the graph it can be seen that at cell size 1.1 & 1.5 the stress as well as deformation as closer to each other. Hence it will be good if there values are considered for the meshing purpose. But to reduce the computation time and to get better results, cell size is considered as 1.5mm.

Force Calculation for Original Design of Discover Connecting Rod

Force due to Combustion Pressure:

We have equation as,

$$F_g = Utmost\ \ Pressure\ of\ the\ \text{Gas} \times \text{Piston Area}$$

$$F_g = P_{max} \times \frac{\pi D^2}{4}$$

Where, P_{max}= 2MPa

$P_{max}= 2\times10^6$ N/m^2

Hence,

$$F_g = 2 \times 10^6 \times \frac{\pi \text{ x } 0.047^2}{4}$$

$$\mathbf{F_g = 3469.9\ N}$$

$$\mathbf{F_g = 3.4699\ KN}$$

The maximum gas pressure because of combustion is 3.4699 KN.

Force due to Inertia of Reciprocating Masses:

$$F_i = 0.474 \times \left(\frac{2 \times \pi \times 2000}{60}\right)^2 0.027 \text{ x } (\cos 10 + \frac{\cos(2 \times 10)}{3.3823})$$

$$F_i = 0.474 \text{ x } 43864.9 \text{ x } 0.027 \text{ x } 1.2626$$

$$\mathbf{F_i = 708.8021\ N}$$

Load cases applied for proposed case study before optimization

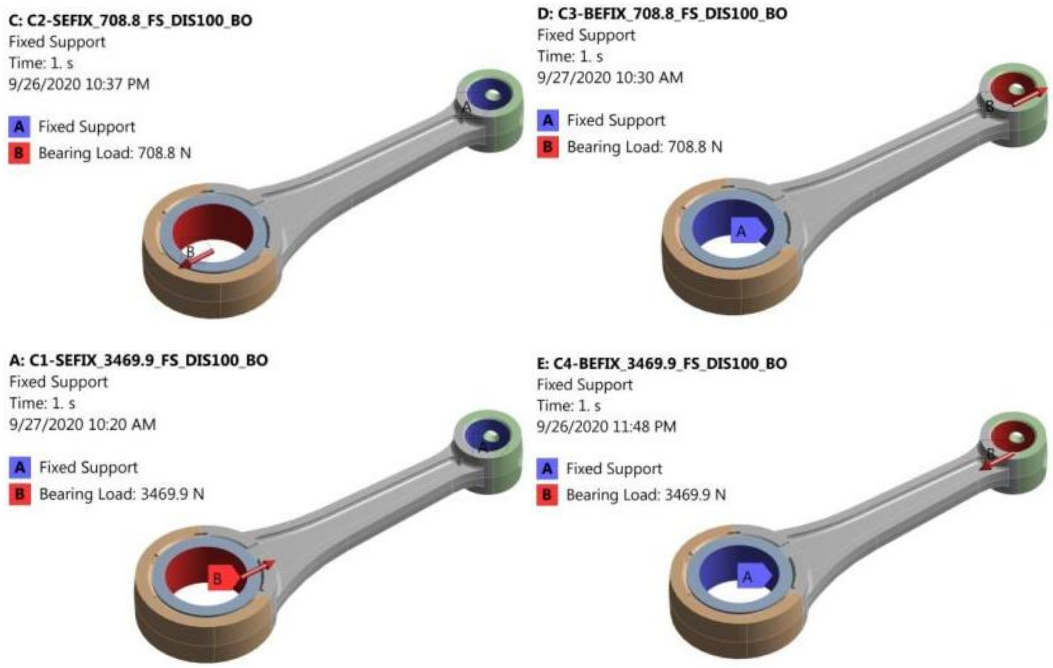

Figure 3: Load Cases applied for case study of Discover connecting rod

Load Case 1: Tensile at crank end (big end).

The maximum tension load taken as highest inertial load. From above equation, maximum tensile load calculated as 708.8 N.

Load Case 1: Boundary Conditions

The maximum tension pressure of 708.8 N applied on inner circumference of crank end (big end) while inner circumference of piston end (small end) is constrained. The calculated maximum tension

pressure 708.8 N applied on inner radial surface of crank end (big end) during analysis, keeping piston end constrained. The constraint & pressure both applied at inner circumference also both applied in radial direction of connecting rod. The constraint applied on nodes, constraining all nodes in radial x-direction.

Load Case 2: Tensile at piston end (small end).

The highest tensile force considered as maximum inertial load. From given equation highest tensile force obtained as 708.8021 N.

Load Case 2: Boundary Conditions:

The highest tensile force of 708.8021 N is exerted on inner periphery of piston end (small end) while inner periphery of crank end (big end) is reserved. The obtained highest tensile force 708.8021 N exerted on inner radial body of piston end (small end) at the time of examination, keeping crank end reserved. The reservations as well as force both exerted at inner periphery also both exerted in axial direction of connecting rod. The reservation exerted on nodes, reserving all nodes in axial x- direction.

Load Case 3: Compression at crank end (big end).

The maximum compressive load considered as maximum gas pressure. From given equation highest compression force obtained as 3469.9 N.

Load Case 3: Boundary condition:

The highest compressive force of 3469.9 N exerted on inner periphery of crank end (big end) while inner periphery of piston end (small end) is reserved. The obtained highest compression force 3469.9 N exerted on inner radial body of crank end (big end) at the time of examination, keeping piston end reserved.

Load Case 4: Compression at piston end (Small End).

The highest compression force taken as highest gas pressure. From above equation, maximum compressive load calculated as 3469.889 N.

Load Case 4: Boundary condition

The maximum compression pressure of 3469.889 N is applied on inner circumference of piston end (small end) while inner circumference of crank end (big end) is constrained. The calculated maximum compressive pressure 708.8021 N applied on inner radial surface of piston end (small end) during analysis, keeping crank end constrained.

4. Result

Static investigation - outcome for discover connecting rod for aluminium material.

Static analysis – finding of total deformation for discover connecting rod, for aluminium material.

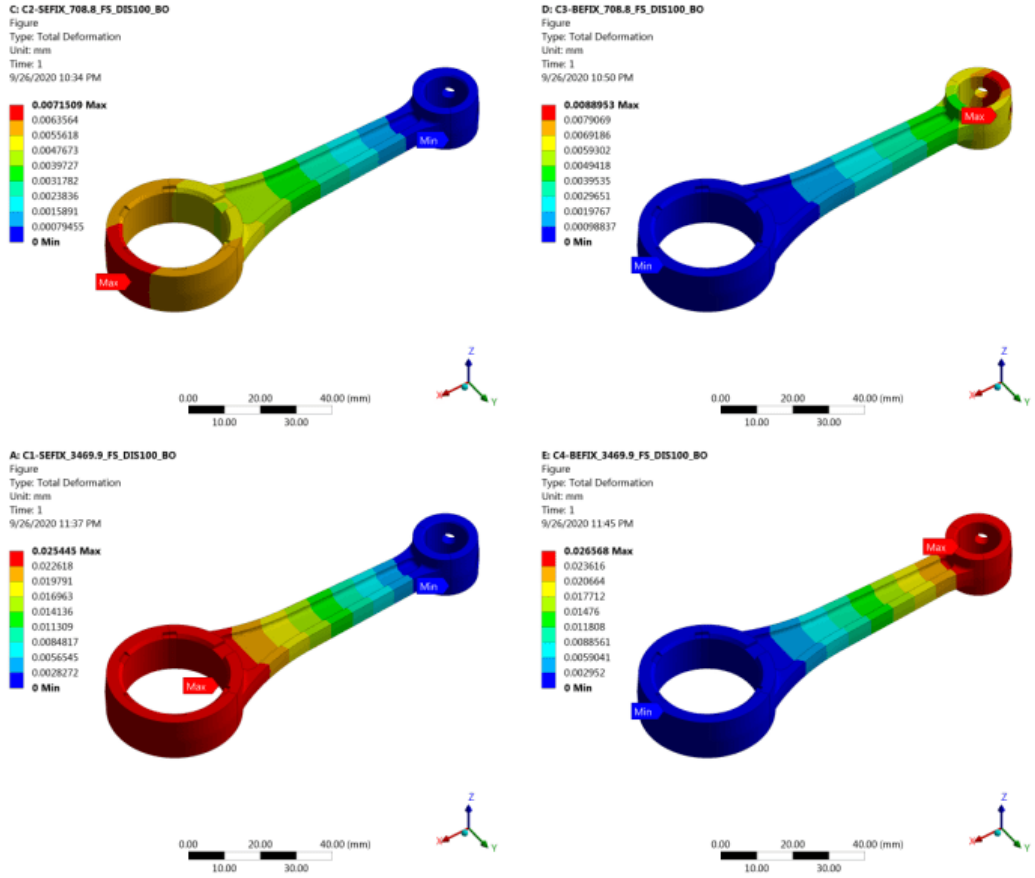

Figure 4: Total Deformation Diagram for Aluminium Material

Load Case 01: Total deformation static examination - result for aluminium material.

While stretchable pressure applied at big end, locality of top most as well as bottom most total deformation noticed from total deformation figure as shown in figure of aluminum. When the stretchable exertion of magnitude 708.8 N is deployed at big as well as small end was reserved, then region of topmost total deformation can be noted as 0.0169490, while bottom most total deformation was noted as 0 for aluminum.

Load Case 02: Total deformation static inspection - outcome for aluminium material.

When tensile effort applied at small end, then location of maximal and minimal total deformation identified from total deformation sketch as shown in figure of aluminum. When the tensile pressure of amount 708.8 N is deployed at small and big end was constrained, then section of maximal total deformation can be noted as 0.0210550, while minimal total deformation was noted as 0 for aluminum.

Load Case 03: Total deformation static analysis - conclusion for aluminium material.

At time of compressive exertion is applied at crank end, the region of highest as well as lowest total deformation can be seen from total deformation outline as shown in figure of aluminum. Locality of highest total deformation can be noted as 0.0603060, while lowest total deformation was noted as 0 for aluminum. The locality of highest total deformation identified in the location near crank end, while lowest total deformation can be identified in the region away from crank end.

Load Case 04: Total deformation static investigation - finding for aluminium material.

During compression, force applied at piston end, section of maximum and minimum total deformation observed from total deformation diagram as shown in figure of aluminum. When the compression effort of magnitude 3469.9 N applied at piston end & crank end inhibited, then location of maximum total deformation noted as 0.0629510.

Static investigation – result of equivalent stress for discover connecting rod, for aluminium material.

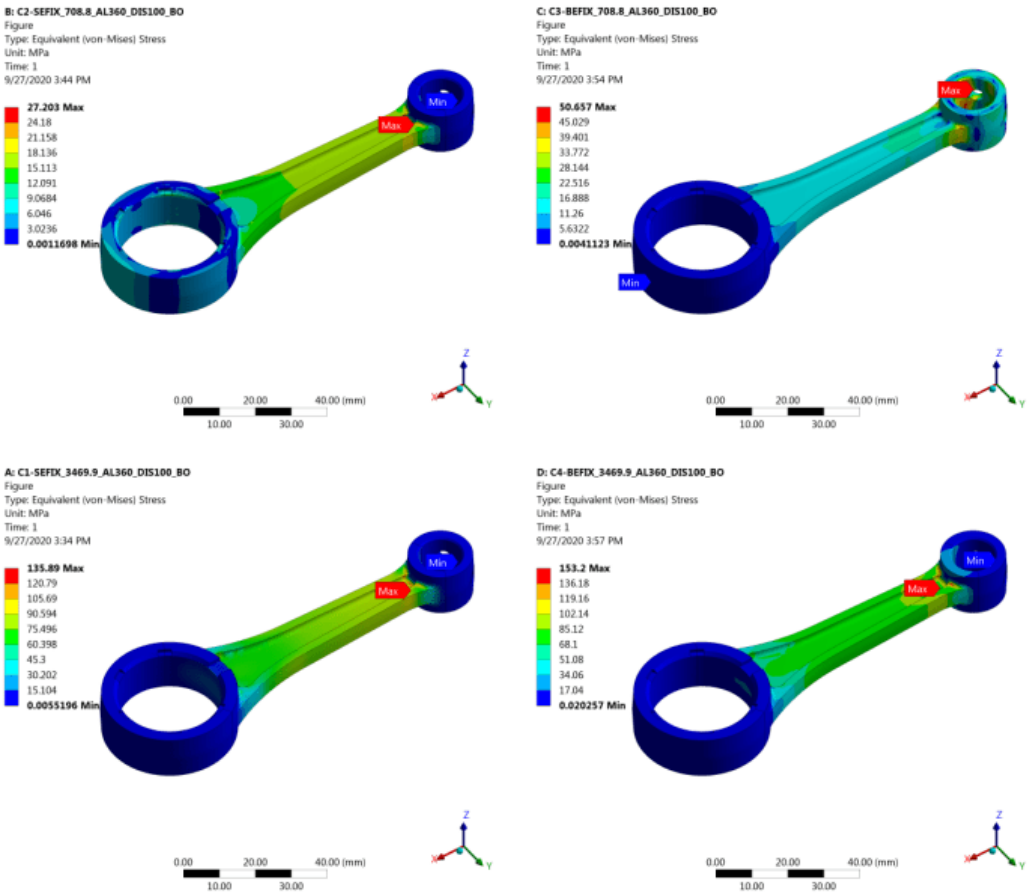

Figure 5 : equivalent stress for Aluminium Material

Load Case 05: Equivalent stress static inspection - outcome for aluminium material.

At time of stretchable pressure applied at big end, then region of top most as well as bottom most equivalent stress observed from equivalent stress figure as shown in figure of aluminum.

When the stretchable pressure of magnitude 708.80 N deployed at big as well as small end guarded, region of top most equivalent stress noted as 27.2 MPa, whereas 0.00116980 MPa noted as bottom-most equivalent stress for aluminum.

Load Case 06: Equivalent stress static analysis - conclusion for aluminium material.

During tensile effort is applied at small end, then section of maximal and minimal equivalent stress can be noticed from equivalent stress sketch as shown in figure of aluminum. When the tensile effort

of magnitude 708.80 N applied at small end as well as big end inhibited, section of maximal equivalent stress noted as 50.7 MPa, while minimal equivalent stress noted as 0.00411230 MPa for aluminum.

Load Case 07: Equivalent stress static investigation - finding for aluminium material.

While compressive exertion applied at crank end, then locality of highest as well as lowest equivalent stress identified from equivalent stress outline as shown in figure of aluminum. When the compressive exertion of magnitude 3469.90 N deployed at crank as well as piston end reserved, locality of highest equivalent stress noted as 135.9 MPa, while lowest equivalent stress noted as 0.00551960 MPa for aluminum.

Load Case 08: Equivalent stress static examination - result for aluminium material.

When, compression force applied at piston end, then location of maximum and minimum equivalent stress, seen from equivalent stress diagram, as shown in figure of aluminum. When the compression force of magnitude 3469.90 N applied at piston end and crank end was constrained, then location of maximum equivalent stress noted as 153.2 MPa, while minimum equivalent stress noted as 0.02025700 MPa for aluminum.

Static examination – outcome of fatigue life for discover connecting rod, for aluminium material.

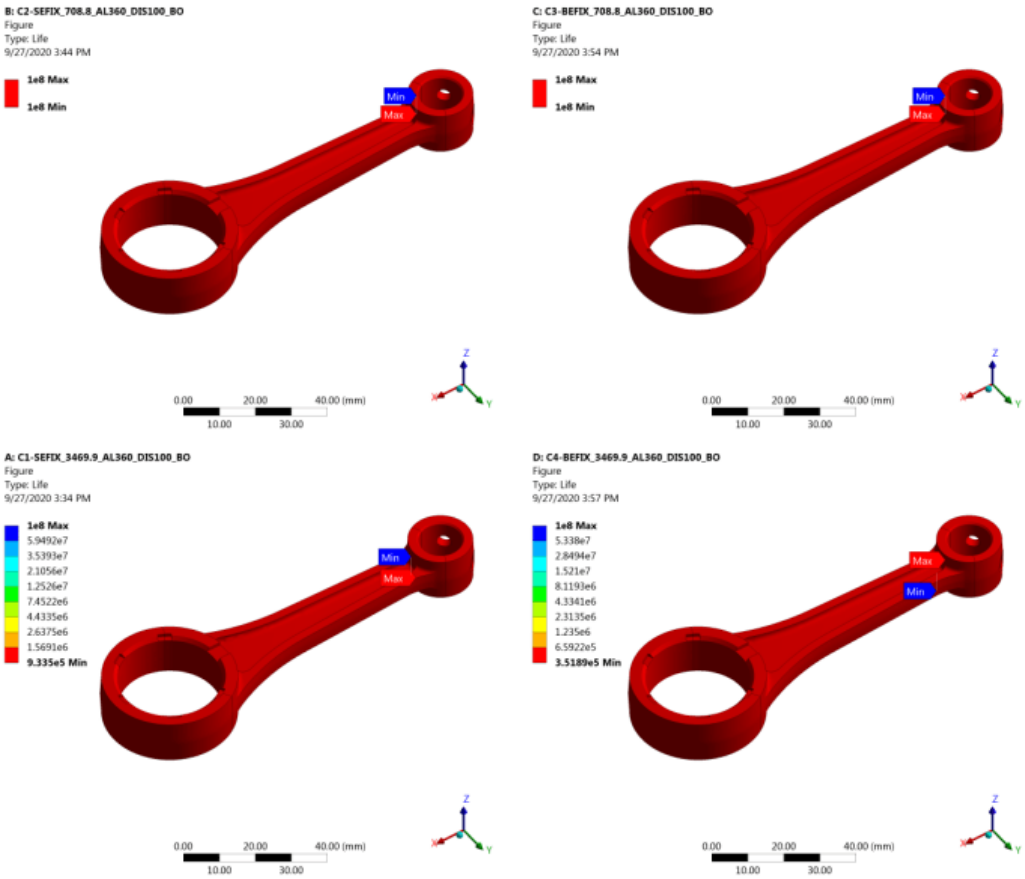

Figure 6: Fatigue Life Diagram for Aluminium Material

Load Case 09: Fatigue life static analysis - conclusion for aluminium material.

When stretchable pressure deployed at big end, then location of top most as well as bottom most fatigue life identified from fatigue life outline as shown in figure of aluminum. When the stretchable effort of magnitude 708.802 N deployed at big as well as small end guarded, and then region of top most fatigue life noted as 1.00 E+08 cycles, while lowest fatigue life noted as 1.000 E+08 cycles for aluminum.

Load Case 10: Fatigue life static investigation - finding for aluminium material.

At time of tensile effort is applied at small end, the region of maximal and minimal fatigue life can be seen from fatigue life diagram as shown in figure of aluminum. When the tensile exertion of magnitude 708.802 N applied, at small end and big end inhibited, then section of maximal fatigue life noted as 1.00 E+08 cycles, while minimum fatigue life, noted as 1.000 E+08 cycles for aluminum.

Load Case 11: Fatigue life static examination - result for aluminium material.

During compressive exertion is applied at crank end, section of highest as well as lowest fatigue life can be observed from fatigue life figure as shown in figure of aluminum. When the compressive force of magnitude 3469.889 N is applied at crank end & piston end was reserved, then locality of highest fatigue life can be noted as 1.00 E+08 cycles, while bottom most fatigue life was noted as 9.335 E+05 cycles for aluminum.

Load Case 12: Fatigue life static inspection - outcome for aluminium material.

While compression force applied at piston end, locality of maximum and minimum fatigue life noticed from fatigue life sketch as shown in figure of aluminum.

When the compression pressure of magnitude 3469.889 N applied at piston end as well as crank end was constrained, and then location of maximum fatigue life noted as 1.00 E+08 cycles, while minimal fatigue life noted as 3.519 E+05 cycles for aluminum.

Static inspection – conclusion of safety factor for discover connecting rod, for aluminium material.

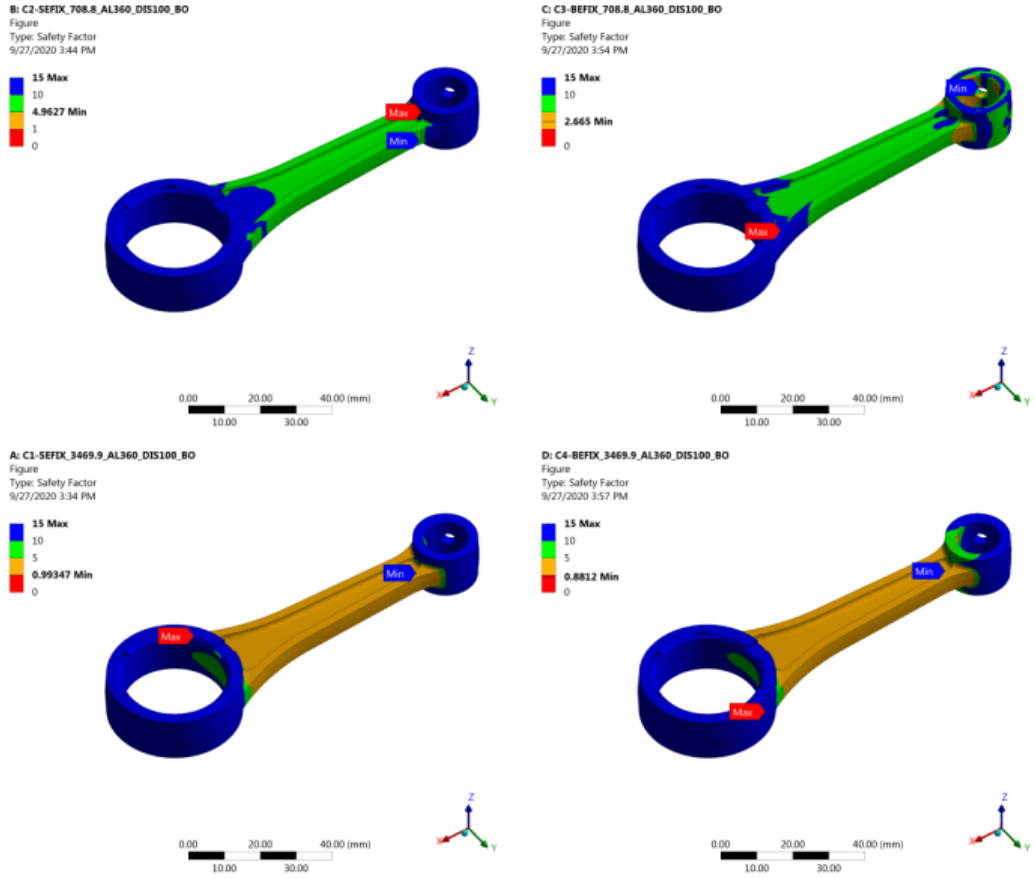

Figure 7: Safety Factor Diagram for Aluminium Material

Load Case 13: Safety factor static investigation - finding for aluminium material.

Topmost safety factor noted as 15.00, whereas 4.9627 noted as lowest safety factor for aluminum.

Load Case 14: Safety factor static examination - result for aluminium material.

During tensile exertion applied at small end, section of top most as well as bottom, most safety factor be noticed from safety factor diagram as shown in figure of aluminum. When the tensile pressure of magnitude 708.8021 N is applied at small end as well as big end was guarded, then section of maximal safety factor can be noted as 15.00, while minimum safety factor was noted as 2.6650 for aluminum.

Load Case 15: Safety factor static inspection - outcome for aluminium material.

While compressive effort applied at crank end, locality of maximal and minimal safety factor identified from safety factor figure as shown in figure of aluminum.

When the compressive effort of magnitude 3469.8890 N is deployed at crank as well as piston end was inhibited, then locality of highest safety factor can be noted as 15.00, while bottom most safety factor was noted as 0.9935 for aluminum. The locality of, highest safety factor; identified in section near crank end. While lowest safety factor, identified in region away from crank end.

Load Case 16: Safety factor static analysis - conclusion for aluminium material.

When, compression pressure, applied at piston end; then location of highest as well as lowest safety factor, seen from safety factor sketch as shown in figure of aluminum. When the compression exertion of magnitude 3469.8890 N is applied at piston end and crank end was reserved, then location of maximum safety factor can be noted as 15.00, while minimal safety factor was noted as 0.8812 for aluminum. The location of, maximum safety factor; seen in the locality, away from piston end. While minimum safety factor seen in the section near piston end.

5. Conclusions

Connecting Rod used in Discover								
	Deformation in mm		Equivalent stress in MPa		Fatigue Life in Cycles		Safety Factor	
Case	Minimum	Maximum	Minimum	Maximum	Minimum	Maximum	Minimum	Maximum
1	0.0	0.0169490	0.0011698	27.203	1.0E+08	1.0E+08	4.9627	15
2	0.0	0.0210550	0.0041123	50.657	1.0E+08	1.0E+08	2.665	15
3	0.0	0.0603060	0.0055196	135.890	9.3E+05	1.0E+08	0.99347	15
4	0.0	0.0629510	0.0202570	153.200	3.5E+05	1.0E+08	0.8812	15

Table 1: Static Analysis Result for Discover Connecting Rod for Aluminum Material

From the Static Analysis - Result for Discover Connecting Rod for Aluminum Material it is found that the minimum Deformation was 0 mm in all the cases and the maximum deformation was in case 4 of 0.0629510 mm. the minimum equivalent stress was in case 1 and it was 0.0011698 MPa whereas the maximum equivalent stress was in case 4 and it was 153.200 MPa. The minimum Fatigue Life was observed as 3.5E+05 cycles in case 4 and the maximum Fatigue Life was observed as 1.0E+08 in all the cases. The minimum safety factor was observed as 0.8812 in case 4 and the maximum safety factor was 15 in all the cases.

References

[1] Mr. Yogesh Kumar Bharti, Mr. Vikrant Singh, Mr. Afsar Hussain, Mr. Dipanshu Singh, Mr. Shyam Bihari Lal and Mr. Satish Kumar Dwivedi (2013), Stress analysis and optimization of connecting rod using finite element analysis, International Journal of Scientific & Engineering Research, Volume No. 4, Issue No. 6, Page No. 15-25

[2] Mr. Yogesh R. Kchrola and Mr. Nelvin Johny (2017), Analysis of Connecting Rod for Various Composite Materials, International Conference on Ideas, Impact and Innovation in Mechanical Engineering (ICIIIME 2017), Volume No. 5, Issue No. 6, Page No. 25-30

[3] Mr. Yong-fei WANG, Mr. Sheng-dun ZHAO and Mr. Chen-yang ZHANG (2017), Microstructures and mechanical properties of semi-solid squeeze casting ZL104 connecting rod, Science Direct - Transaction of Nonferrous Metals Society of China, Volume No. 12, Issue No. 3, Page No. 211–220

[4] Mr. Yoo Y. M., Mr. Haug E. J. and Mr. Choi K. K. (1984), Shape optimal design of an engine connecting rod, Journal of Mechanisms, Transmissions, and Automation in Design, Transactions of ASME, , Volume No. 106, Issue No. 2, Page No. 415-419

[5] Mr. Zhiwei Tong, Mr. Hao Liu and Mr. Fengxia Zhu (2009), Modal Analysis for Connecting Rod of Reciprocating Mud Pump, Springer-Verlag Berlin Heidelberg, Volume No. 21, Issue No. 3, Page No. 215–220

[6] Mrs. Dipalee S. Bedse (2017), Design Evaluation of Connecting Rod, International Journal of Recent Engineering Research and Development (IJRERD), Volume No. 2, Issue No. 7, Page No. 203-213

[7] Mrs. Dipalee S. Bedse and Mr. Mangesh. A. Ahire (2015), Design Evaluation Through Finite Element Analysis For Fatigue Life Of Connecting Rod Used In Two Wheelers, International Journal of Advanced Technology in Engineering and Science, Volume No. 3, Issue No. 1, Page No. 26-40

[8] Mr. Prathamesh S. Gorane and Dr. Kashinath H. Munde, Analysis and Optimization of a Connecting Rod (2020), IJSRD - International Journal for Scientific Research & Development, Vol. 8, Issue 9, 2020, ISSN (online): 2321-0613

[9] Mr. Prathamesh S. Gorane and Dr. Kashinath H. Munde, Finite Element Analysis of Optimized Connecting Rod (2020), IJSRD - International Journal for Scientific Research & Development, Vol. 8, Issue 9, 2020, ISSN (online): 2321-0613

[10] Dr. Prathamesh S. Gorane and Dr. Vijay B. Roundal, Connecting Rod Design along with Analysis a Review (2022), Journal of Automation and Automobile Engineering, e-ISSN: 2582-3159, Volume-7, Issue-1 (January-April, 2022).

[11] Dr. Vijay B. Roundal & Dr. Prathamesh S. Gorane, Free vibration analysis for Dynamic Stiffness formulation-Literature review (2022), Journal of Mechanical and Mechanics Engineering, e-ISSN: 2581-3722, Volume-8, Issue-1 (January-April, 2022)